

Communication

Effective Harmful Organism Management I: Fabrication of Facile and Robust Superhydrophobic Coating on Fabric

Chang-Ho Choi ¹, Yeongwon Kwak ¹, Min Kyung Kim ² and Dong Gun Kim ^{3,*} 

¹ Department of Chemical Engineering, Gyeongsang National University, Jinju 52828, Korea; ch_choi@gnu.ac.kr (C.-H.C.); hyjk755@gnu.ac.kr (Y.K.)

² Department of Bio & Environment Technology, Seoul Women's University, Seoul 01797, Korea; min4190@naver.com

³ Smith College of Liberal Arts, Sahmyook University, Seoul 01795, Korea

* Correspondence: ecology@syu.ac.kr; Tel.: +82-2-3399-1919

Received: 30 May 2020; Accepted: 18 July 2020; Published: 22 July 2020



Abstract: Advances in harmful organism management are highly demanding due to the toxicity of conventional coating approaches. Exploiting biomimetic superhydrophobicity could be a promising alternative on account of its cost-effectiveness and eco-friendliness. Here, we introduce a facile method to fabricate a robust superhydrophobic coating on a fabric substrate. This is achieved by sequentially spraying TiO₂-epoxy resin nanocomposite material and fluorocarbon-silane modified SiO₂ nanoparticles (FC-silane SiO₂ NPs). The superhydrophobicity is attributed to the nanoparticles constituting a micro/nano hierarchical structure and the fluorocarbon of the modified SiO₂ NPs lowering the surface energy. The epoxy resin embedded in the coating layer plays an important role in improving the robustness. The robustness of the superhydrophobic surface is demonstrated by measuring the water slide angle of surfaces that are subject to salty water at 500 rpm stirring condition for up to 13 days. This study focuses on ensuring the superhydrophobicity and robustness of the coating surface, which is preliminary work for the practical management of macrofoulers. Based on this work, we will perform practical harmful organism management in seawater as a second research subject.

Keywords: superhydrophobic; fabric substrate; robustness; fluorocarbon-silane modified SiO₂ NPs

1. Introduction

The introduction of alien or invasive species, such as microorganisms, plants, algae, or small animals, into land or water ecosystems has been recognized as a major problem since the last century [1]. These invasive species act as vectors for new diseases, alter ecosystem processes, reduce biodiversity, and lead to major economic losses [2]. For instance, it was reported that invasive invertebrate species have spread widely through maritime activities by attaching to ship hulls and surviving in ballast water [3–6]. These benthic invertebrate species release planktonic larvae or spores that may attach to new substrata for possible recruitment [7]. This characteristic is called biofouling or biological fouling. Common macrofoulers include macroalgae sponges, hydroids, bryozoans, some polychaetes, barnacles, mussels, and some ascidians [7]. Biofouling causes many problems in aquaculture such as fouling on infrastructure (cages, netting, pontoons, and buoys) and stock species (farmed species including mussels, scallops, oysters, and fishes) [8]. In addition, these macrofoulers can increase the fuel consumption of a ship and sailing time with its attendant costs [9]. Therefore, many antifouling methods have been developed, including physical, chemical, and biological methods [10–13]. One representative approach for antifouling is to employ antifouling paint for maintenance of vessels and marine structures.

However, residues of the antifouling paint could be generated and exposed to sediment layers in aquatic systems, which eventually leads to a potential threat to benthic invertebrates [14]. Another conventional method for the antifouling effect is to coat antifouling substances based on copper and/or organotin compounds [15]. The toxicity of these compounds has been reported along with their long persistence in the environment and their harmful impact on sea life as well. Because of the environmental hazard in the conventional antifouling methods, eco-friendly techniques based on engineering nanomaterials have been increasingly developed. For example, encapsulating biocide inside silica mesoporous nanocapsules (SiNC) successfully enabled tailored release of biocide over time, lowering the environmental hazard as compared to its free form [16]. Recently, biomimetic antifouling strategies have been widely investigated owing to their cost-effectiveness and eco-friendliness [17]. A key feature of biomimetic antifouling is to mimic the “Lotus Effect” in which superhydrophobic surfaces are established. The superhydrophobic nature provides an excellent self-cleaning, anti-icing, and antifouling function [18,19]. Since the combination of micro/nano dual-scale structure and low surface energy are attributed to the superhydrophobic nature, various methods have been attempted to fabricate micro/nano hierarchical structures with low surface energy [20]. Although synthetic methodologies and coating techniques for constructing a superhydrophobic surface have consistently evolved, the practical examination of a superhydrophobic surface for harmful organism management is scarce. In order to realize effective harmful organism management, the superhydrophobic coating material and coating method should first be developed, along with the robustness acquisition of the coating material.

Here, we introduce a facile strategy to fabricate a robust superhydrophobic coating on fabric substrate for potential application of the effective management of macrofoulers. There are many coating methods to build the micro/nano structure, including dip-coating, spin-coating, drop-casting, and spray coating. Among these, a spray coating method is the most suitable for superhydrophobic coating due to its simplicity and, in particular, its ability to enable large-scale deposition [20]. The substrate should also be selected by considering practical harmful organism management, which could involve an aquaculture farm, harbor, or ship hull [21]. In this regard, fabric can be a good option as a substrate since the flexibility of the fabric texture allows for excellent processibility. Therefore, we fabricated a superhydrophobic surface on a fabric substrate by using the spray method. The coating is prepared by two-step spray deposition in which the first layer consisting of TiO₂-epoxy resin nanocomposite is deposited and subsequently fluorocarbon-silane modified SiO₂ nanoparticles (FC-silane SiO₂ NPs) are applied onto the first layer. SiO₂ NPs are chemically functionalized by fluorocarbon to lower the surface energy. The functionalized silica NPs serve as the constitution of a micro-nano dual structure while the epoxy resin improves the robustness of the coating. The superhydrophobic nature of the coating is demonstrated by the near zero degree water slide angle. For the robustness evaluation, the superhydrophobic surfaces are subject to water and salty water at 500 rpm stirring condition for up to 13 days. The evaluation results prove the sufficient robustness of the surface for real harmful organism management.

2. Materials and Methods

2.1. Materials

Titanium (IV) oxide (anatase, powder, 99.8%), Trichloro (1H,1H,2H,2H-perfluorooctyl) silane (PFOCTS), and SiO₂ NPs (~20 nm in diameter) were purchased from Sigma Aldrich. 1-propanol (99.5%) and acetone (99.5%) solvent were purchased from JUNSEI Chemical Co., Ltd. and SAMCHUN Chemical Co., Ltd., respectively. Epoxy resin and hardener were purchased from Dasol Chemical Co., Ltd. The main component of the epoxy resin and hardeners is 2,2-bis (4'-glycidioxyphenyl) propane (diglycidyl ether of bisphenol A) and trimethylolpropane poly (oxypropylene) triamine, respectively. The material of the fabric substrate is cotton. All the materials were used as received without further purification.

2.2. Fabrication of Superhydrophobic Surface

In order to fabricate the superhydrophobic surface, SiO₂ NPs were first functionalized with fluorocarbon. The functionalization process was carried out as described in a previous work [22]. Briefly, 2 g of SiO₂ NPs and 1 mL PFOCTS were dispersed in toluene (40 mL). The mixture was refluxed for 3 h to produce FC-silane SiO₂ NPs. After the reflux, the FC-silane SiO₂ NPs were washed with EtOH by centrifugation several times. The FC-silane SiO₂ NPs were dried at 70 °C in an oven. The first coating material solution was prepared by mixing TiO₂ NPs (0.83 g), epoxy resin (0.5 g), and hardener (0.25 g) in acetone solvent (4 mL). The mixing process proceeded for 30 min at 500 rpm. The homogeneous solution was then sprayed on the fabric substrate by using an airbrush, keeping the distance of ~30 cm between the substrate and the airbrush. After coating the first layer on the substrate, the sample was placed in a thermal oven set to 70 °C for 3 h for the curing of the epoxy resin. The second coating material was prepared by mixing the FC-silane SiO₂ NPs (0.05g) in propanol solvent (5 mL). The solution was then treated with sonication for 30 min. Similar to the first coating material deposition, the second coating solution was sprayed onto the first coating layer using the same airbrush. The surface was then subject to the second curing at 70 °C for 3 h. The areal density of the TiO₂-epoxy composite and FC-silane SiO₂ NPs was around 140 and 7.84 g m⁻², respectively.

2.3. Characterization of Superhydrophobic Surface

Morphology of the pristine and coated surface was examined by using a field-emission scanning electron microscope (FE-SEM, JEOL, JSM-7610F). The elemental mapping of the coated surface was performed by using energy-dispersive X-ray spectroscopy (EDS) equipped with SEM. Chemical functionality of FC-silane SiO₂ NPs was determined by using Fourier transform infrared spectroscopy (FT-IR, Thermo Fisher, IS50). Superhydrophobicity was evaluated by measuring the water slide angle. A water droplet of 10 µL was placed on a surface that was inclined at a certain angle. The distance between the droplet position and the test surface was maintained at about 10 cm. The water slide angle was measured at the moment when the droplet rolled off.

2.4. Robustness Evaluation of Superhydrophobic Surface

For the robustness evaluation of the surface, we prepared a total of 48 pieces of the superhydrophobic surfaces (each piece is 2.5 cm × 2.5 cm). As shown in the setup for the robustness evaluation (Figure S1), 24 pieces of the surfaces were immersed in a deionized (D.I.) water bath, and the other 24 pieces were immersed in a salty water (35 ppt) bath. The salty water with 35 ppt was prepared by dissolving 35 g of sodium chloride in 1000 mL D.I. water. The superhydrophobic surfaces were kept subject to 500 rpm stirring condition at room temperature for up to 13 days. Three surfaces were taken out from each bath every two days for the robustness test. The robustness of the surfaces was evaluated by taking an average water slide angle of three samples.

3. Results and Discussion

Figure 1 shows a series of SEM images of a pristine fabric substrate and superhydrophobic surface. The pristine fabric substrate initially with a beige color turned into one with a white color after the coating (inset of Figure 1a,b). In consideration of the coating material solution having the white color, the color change from beige to white implies the successful deposition of the coating materials on the fabric substrate (Figure S2). The SEM comparison in Figure 1a,b reveals that a bundle of fabrics of the pristine substrate was uniformly deposited with the coating materials after the coating. The SEM images with higher magnification also exhibit the distinct morphological change of the fabric surface after the coating (Figure 1c,d). While the bundle of fabric shows a smooth texture, the coated fabric is highly rough. In the cross-sectional SEM image of the coated surface, two boundaries are clearly observed on the fabric substrate (Figure 1e). This is because the fabrication of a superhydrophobic surface is based on the two-step process in which the TiO₂-epoxy nanocomposite solution was first

sprayed on the substrate, and after 3 h curing time the second coating material with FC-silane SiO₂ NPs was applied on the first coating layer. The 3 h time elapse between the first and second spray coating is necessary. Otherwise, the rheology of the first nanocomposite layer is not appropriate for the imposition of the second spray coating. Indeed, if the curing time was shorter than 3 h, the first coating layer partially peeled off during the spray of the second coating solution. In the case of curing time exceeding 3 h, on the other hand, the epoxy resin in the nanocomposite layer was completely cured prior to the deposition of the second coating material, which would result in the loss of the adhesive function of the epoxy resin. In order to clarify the role of each component, we fabricated various samples including TiO₂-epoxy nanocomposite on the fabric, FC-silane SiO₂ NPs/epoxy resin on the fabric, and FC-silane SiO₂ NPs/TiO₂ NPs on the fabric. In the TiO₂-epoxy nanocomposite only on the fabric, the epoxy resin encompasses the TiO₂ NPs, and the nanocomposite is uniformly deposited on an entire bundle of the fabric (Figure S3). The nanocomposite layer showed a hydrophilic property with a wetting behavior in which a water droplet permeated into the fabric (Figure S3). This demonstrates that using FC-silane SiO₂ NPs is essential for the preparation of the superhydrophobic surface. There are many reports on the utilization of FC-silane SiO₂ NPs to produce superhydrophobic surfaces [23–27]. The role of TiO₂ NPs was clarified according to the SEM analysis of the FC-silane SiO₂ NPs/epoxy resin sample (Figure S4). In the absence of the TiO₂ NPs, the flexibility of the fabric substrate was completely lost. This is because the epoxy resin totally filled inside pores between fabrics and formed a continuous epoxy film, which is opposed to the TiO₂-epoxy nanocomposite sample. As briefly mentioned earlier, the flexibility of our superhydrophobic surface is a very critical aspect in terms of the versatile processibility for practical harmful organism management. For example, the superhydrophobic fabric could be readily secured on a buoy or harbor wall. The superhydrophobic fabric also provides structural flexibility meaning that objects with any shape could be covered by the fabric. The easy replacement and low cost are other advantages of the fabric substrate. The role of epoxy resin as an adhesive was also confirmed during the fabrication process. In the absence of the epoxy resin, the TiO₂ NPs were not tightly adhered on the fabric, and thus during the second coating of the FC-silane SiO₂ NPs, the pre-sprayed TiO₂ NPs were partially detached from the fabric substrate. It was reported that epoxy resin can serve as an adhesive for the fabrication of superhydrophobic coatings [28]. The epoxy resin embedded inside the coating layer causes the coated surface to be stiff, but the surface recovers most of its flexibility after bending several times. Even after the bending of the coated surface several times, its superhydrophobicity remains the same, indicating that the superhydrophobic coating materials rigidly stick to the fabric texture. The coating layers are non-uniform in thickness because the fabric substrate itself is non-uniform, as shown in Figure 1a. A top-view SEM image shows that the superhydrophobic coating consists of a micro/nano hierarchical structure (Figure 1f). The nanostructure was built by SiO₂ NPs of around 20 nm in diameter, and the microstructure would be formed by random aggregation of SiO₂ NPs. These results clearly indicate that the presence of TiO₂ NPs, epoxy resin, and FC-silane SiO₂ NPs is essential to produce the robust superhydrophobic fabric with high flexibility. The components of the superhydrophobic surface are confirmed by the EDS analysis (Figure 1g). All of the major elements forming the coating layers are homogeneously detected over the superhydrophobic surface, including oxygen (O), fluorine (F), silicon (Si), and titanium (Ti). All these characterization results demonstrate the successful deposition of the superhydrophobic coating layer over the entire area of the fabric substrate.

Fluorocarbon is known to play a critical role in effectively reducing the surface energy and thus it is widely employed for the preparation of a superhydrophobic surface [29]. SiO₂ NPs functionalized with fluorocarbon were further analyzed by using FT-IR spectroscopy (Figure 2). There are three peaks commonly observed from both the functionalized SiO₂ NPs and pristine SiO₂ NPs. Two strong peaks at 1100 and 480 cm⁻¹ correspond to the asymmetric stretching vibration of Si-O-Si bonds and the rocking vibration of Si-O-Si bonds, respectively [30,31]. Another peak at around 800 cm⁻¹ is attributed to the bending mode of Si-O-Si bonds [25]. All of the three peaks are associated with SiO₂ NPs. The peaks corresponding to fluoro-carbon bonds are only observed from the functionalized SiO₂

NPs (dotted circle). Some weak peaks located between 700 and 780 cm^{-1} represent fluoro-carbon bonds, proving the successful functionalization of SiO_2 NPs with fluorocarbon [32,33]. Another small peak at approximately 900 cm^{-1} can be assigned to the C-H bonds in the PFOCTS [25].

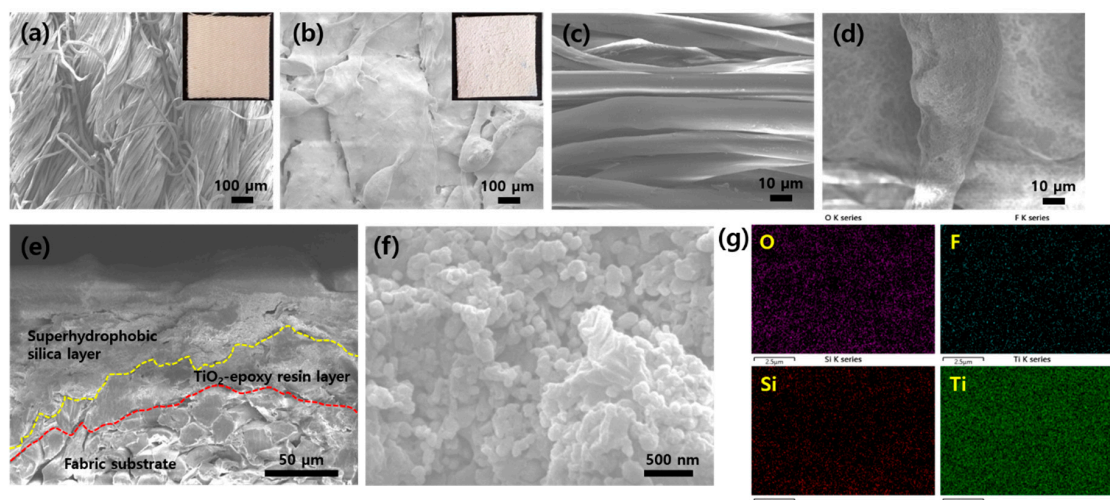


Figure 1. SEM images of (a) pristine fabric substrate (inset: optical image of fabric substrate) and (b) coated surface (inset: optical image of coated surface); (c) pristine fabric substrate and (d) coated surface with higher magnification; (e) cross-sectional view and (f) plain view of coated surface; and (g) EDS analysis for elemental mapping.

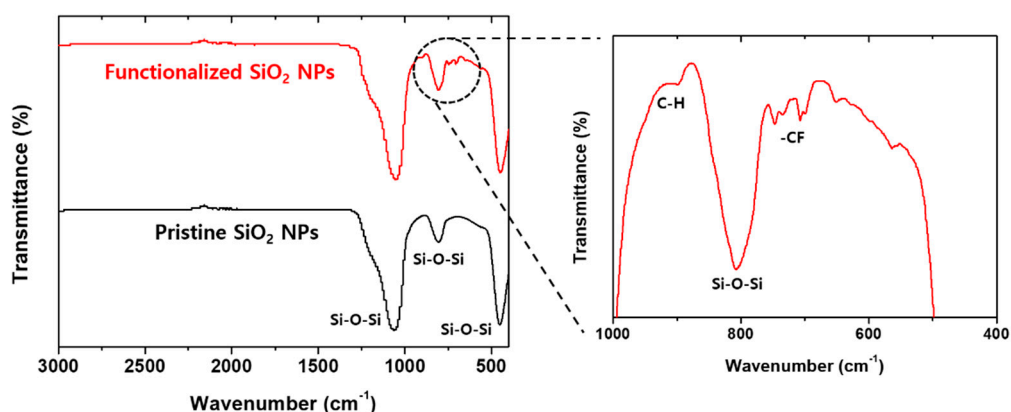


Figure 2. FT-IR spectra comparison of functionalized SiO_2 NPs and pristine SiO_2 NPs.

Figure 3a compares the shapes of water droplets placed on the pristine fabric substrate and on the coated surface (the droplet was dyed with phenolphthalein for clarification). The water droplet on the coated surface is more spherical than the pristine one, demonstrating the higher water repellency of the coated surface as compared to the pristine fabric substrate. For a dramatic water repellency comparison of the surfaces, several water droplets were placed onto the pristine and coated substrates. While the droplets on the pristine substrate firmly clung onto the substrate even upside down, those placed on the coated surface immediately bounced off (Videos S1 and S2). The coated substrate showed a near zero degree water slide angle, as opposed to the pristine one from which the droplet did not roll off even upside down (Videos S2 and S3). Lastly, we immersed the pristine and coated substrates in a water bath to prove the air entrapment of the coated substrate (Figure 3b). The formation of an air blanket was clearly observed over the coated substrate, contrary to the pristine one. The air entrapment is a key feature of superhydrophobic surfaces and is well explained by the Cassie–Baxter model [19]. All these comparison results support the superhydrophobic nature of the coated surface.

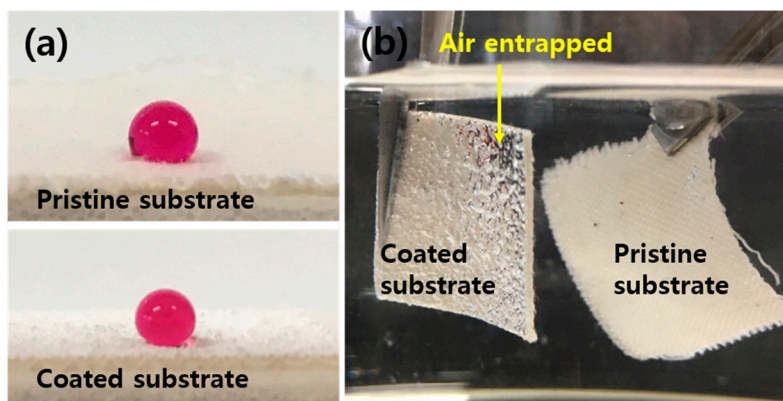


Figure 3. (a) Optical image comparison of dyed water droplet on pristine and coated substrates and (b) air entrapment test of coated substrate.

We evaluated the robustness of the superhydrophobic surface by periodically measuring the water slide angle of surfaces that were immersed in D.I. water and salty water (35 ppt) at 500 rpm stirring condition at room temperature, which approximately corresponds to shear stress of 8.9×10^{-4} Pa (Figure S1). The robustness test results of the superhydrophobic surfaces are exhibited in Figure 4. In the D.I. water test, the water slide angle of all the tested substrates was measured at below 3° regardless of the test period. A water slide angle of 10° is a general criterion to judge superhydrophobicity [34]. Comparing the near zero degree water slide angle (0.6°) of the as-coated surface with 1.9° for the 13 days tested surface, it is believed that little damage was exerted on the coated surface during the test period. In the salty water (35 ppt) test, the slide angle was slightly increased from 0.6° to 3.6° after the test period of 13 days. Considering that the slide angle was maintained below 2° up to 11 days, the coated surface may begin to be slightly damaged after 11 days in the salted water condition. However, the slide angle of 3.6° is still much lower than the criterion angle (10°) of superhydrophobicity. The superhydrophobic surface tested for 13 days was examined by SEM and EDS. No noticeable morphological change was observed after the robustness test, and the fluorine element was also detected uniformly over the surface. This supports the retention of the superhydrophobicity of the sample even after the 13-day test period (Figure S5). A series of water droplets taken at each test period are also included in Figure 4. All of the water droplets retained the spherical shape regardless of the test period, corresponding to the results of the water slide angle measurement. The fact that the tested surfaces can sustain their superhydrophobicity during the test period obviously demonstrates the sufficient robustness of the coated surface for harmful organism management. Based on these promising results, we will apply the superhydrophobic surface for aqua ecosystems, further investigate ecological traits of macrofoulers, and eventually develop an advanced coating material for real harmful organism management.

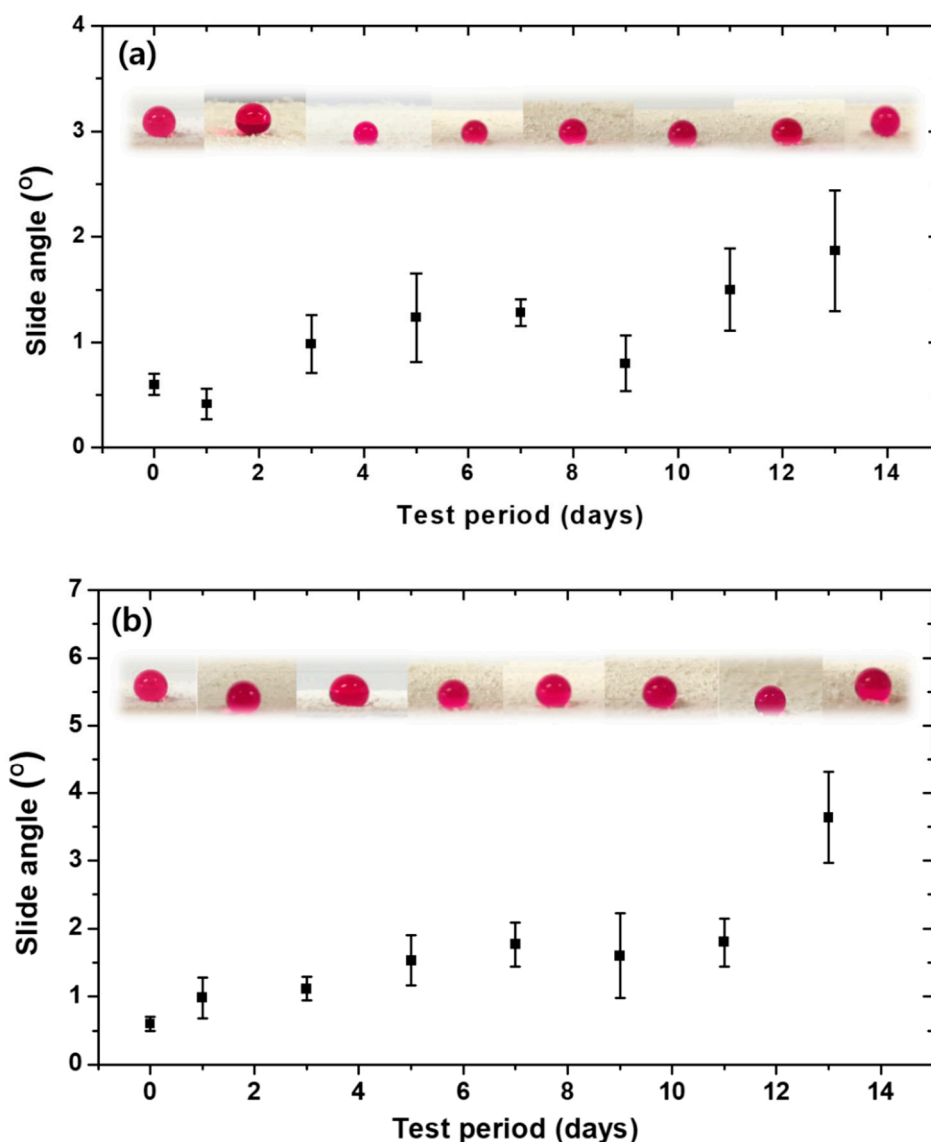


Figure 4. Water slide angle measurement as a function of test period up to 13 days in (a) D.I. water and (b) salted water (35 ppt) at 500 rpm stirring condition at room temperature.

4. Conclusions

A robust superhydrophobic coating was fabricated on a fabric substrate in a facile two-step coating process. The first coating layer was made by spraying a TiO₂-epoxy resin nanocomposite material on the substrate, and subsequently FC-silane SiO₂ NPs were sprayed on the first coating layer. The SiO₂ NPs constituted a micro/nano hierarchical structure, and the fluorocarbon of the functionalized SiO₂ NPs lowered surface energy. This morphological and chemical integration led to a superhydrophobic surface with a near zero degree water slide angle. The epoxy resin contained in the first coating material enhanced the robustness of the coated surface to the extent that the coated surface could sustain its superhydrophobicity in salty water at 500 rpm stirring condition for 13 days. This facile and robust superhydrophobic coating may offer an alternative to conventional harmful organism management.

Supplementary Materials: The following are available online at <http://www.mdpi.com/2071-1050/12/15/5876/s1>, Figure S1: Robustness evaluation of the superhydrophobic surfaces, Figure S2: Optical image of the coating material solution, Figure S3: SEM Images of TiO₂-epoxy nanocomposite on fabric, Figure S4: SEM Images of FC-silane SiO₂ NPs / epoxy resin on fabric, Figure S5: SEM and EDS images of the superhydrophobic surface after the robustness test, Video S1: Water droplet behavior on the pristine fabric, Video S2: Water droplet behavior on the coated fabric, Video S3: roll off of water droplets on the coated fabric.

Author Contributions: C.-H.C. and D.G.K. conceived and designed experiments, guided the data collection and analysis, and wrote the manuscript. Y.K. and M.K.K. conducted the experiments and collected and characterized the data. All authors have read and agreed to the published version of the manuscript.

Funding: This work was supported by a National Research Foundation of Korea (NRF) grant funded by the Korea government (No. 2019R111A3A01058865).

Conflicts of Interest: The authors declare no conflict of interest.

References

1. Bax, N.; Carlton, J.; Mathews-Amos, A.; Haedrich, R.; Howarth, F.; Purcell, J.; Rieser, A.; Gray, A. The control of biological invasions in the world's oceans. *Conserv. Biol.* **2001**, *15*, 1234–1246. [[CrossRef](#)]
2. Mack, R.N.; Simberloff, D.; Mark Lonsdale, W.; Evans, H.; Clout, M.; Bazzaz, F.A. Biotic invasions: Causes, epidemiology, global consequences, and control. *Ecol. Appl.* **2000**, *10*, 689–710. [[CrossRef](#)]
3. Monniot, C.; Monniot, F. Additions to the inventory of eastern tropical Atlantic ascidians; arrival of cosmopolitan species. *Bull. Mar. Sci.* **1994**, *54*, 71–93.
4. Lambert, C.C.; Lambert, G. Persistence and differential distribution of nonindigenous ascidians in harbors of the Southern California Bight. *Mar. Ecol. Prog. Ser.* **2003**, *259*, 145–161. [[CrossRef](#)]
5. Ruiz, G.M.; Fofonoff, P.W.; Carlton, J.T.; Wonham, M.J.; Hines, A.H. Invasion of coastal marine communities in North America: Apparent patterns, processes, and biases. *Annu. Rev. Ecol. Syst.* **2000**, *31*, 481–531. [[CrossRef](#)]
6. Kim, M.K.; Kim, D.H.; Park, J.-U.; Kim, D.H.; Yoon, T.J.; Kim, D.G.; Lee, Y.; Shin, S. Effects of temperature and salinity on the egg development and larval settlement of *Ciona robusta* (Ascidacea, Phlebobranchia, Cionidae). *Ocean. Sci. J.* **2019**, *54*, 97–106. [[CrossRef](#)]
7. Phillippi, A.L.; O'Connor, N.J.; Lewis, A.F.; Kim, Y.K. Surface flocking as a possible anti-biofoulant. *Aquaculture* **2001**, *195*, 225–238. [[CrossRef](#)]
8. Park, J.; Lee, T.; Kim, D.; Kim, P.; Kim, D.G.; Shin, S. Monitoring and impact of marine ecological disturbance causing organisms on an oyster and sea squirt farm. *Korean J. Environ. Biol.* **2017**, *35*, 677–683. [[CrossRef](#)]
9. Demirel, Y.K.; Uzun, D.; Zhang, Y.; Fang, H.-C.; Day, A.H.; Turan, O. Effect of barnacle fouling on ship resistance and powering. *Biofouling* **2017**, *33*, 819–834. [[CrossRef](#)]
10. Lafferty, K.D.; Kuris, A.M. Biological control of marine pests. *Ecology* **1996**, *77*, 1989–2000. [[CrossRef](#)]
11. Hodson, S.L.; Lewis, T.E.; Burkea, C.M. Biofouling of fish-cage netting: Efficacy and problems of in situ cleaning. *Aquaculture* **1997**, *152*, 77–90. [[CrossRef](#)]
12. Bellas, J.; Vázquez, E.; Beiras, R. Toxicity of Hg, Cu, Cd, and Cr on early developmental stages of *Ciona intestinalis* (Chordata, Ascidacea) with potential application in marine water quality assessment. *Water Res.* **2001**, *35*, 2905–2912. [[CrossRef](#)]
13. Granmo, Å.; Ekelund, R.; Sneli, J.-A.; Berggren, M.; Svavarsson, J. Effects of antifouling paint components (TBTO, copper and triazine) on the early development of embryos in cod (*Gadus morhua* L.). *Mar. Pollut. Bull.* **2002**, *44*, 1142–1148. [[CrossRef](#)]
14. Soroldoni, S.; da Silva, S.V.; Castro, Í.B.; Martins, C.d.M.G.; Pinho, G.L.L. Antifouling paint particles cause toxicity to benthic organisms: Effects on two species with different feeding modes. *Chemosphere* **2020**, *238*, 124610. [[CrossRef](#)]
15. Yebra, D.M.; Kiil, S.; Dam-Johansen, K. Antifouling technology—Past, present and future steps towards efficient and environmentally friendly antifouling coatings. *Prog. Org. Coat.* **2004**, *50*, 75–104. [[CrossRef](#)]
16. Figueiredo, J.; Loureiro, S.; Martins, R. Hazard of novel anti-fouling nanomaterials and biocides DCOIT and silver to marine organisms. *Environ. Sci. Nano* **2020**, *7*, 1670–1680. [[CrossRef](#)]
17. Selim, M.S.; El-Safty, S.A.; Shenashen, M.A.; Higazy, S.A.; Elmarakbi, A. Progress in biomimetic leverages for marine antifouling using nanocomposite coatings. *J. Mater. Chem. B* **2020**, *8*, 3701–3732. [[CrossRef](#)]
18. Darmanin, T.; Guittard, F. Recent advances in the potential applications of bioinspired superhydrophobic materials. *J. Mater. Chem. A* **2014**, *2*, 16319–16359. [[CrossRef](#)]
19. Das, S.; Kumar, S.; Samal, S.K.; Mohanty, S.; Nayak, S.K. A review on superhydrophobic polymer nanocoatings: Recent development and applications. *Ind. Eng. Chem. Res.* **2018**, *57*, 2727–2745. [[CrossRef](#)]
20. Ghasemlou, M.; Daver, F.; Ivanova, E.P.; Adhikari, B. Bio-inspired sustainable and durable superhydrophobic materials: From nature to market. *J. Mater. Chem. A* **2019**, *7*, 16643–16670. [[CrossRef](#)]

21. Atalah, J.; Hopkins, G.A.; Fletcher, L.M.; Castinel, A.; Forrest, B.M. Concepts for biocontrol in marine environments: Is there a way forward. *Manag. Biol. Invasions* **2015**, *6*, 1–12. [[CrossRef](#)]
22. Ogihara, H.; Xie, J.; Saji, T. Controlling surface energy of glass substrates to prepare superhydrophobic and transparent films from silica nanoparticle suspensions. *J. Colloid Interf. Sci.* **2015**, *437*, 24–27. [[CrossRef](#)] [[PubMed](#)]
23. Huang, C.; Wang, F.; Wang, D.; Guo, Z. Wear-resistant and robust superamphiphobic coatings with hierarchical TiO₂/SiO₂ composite particles and inorganic adhesives. *New J. Chem.* **2020**, *44*, 1194–1203. [[CrossRef](#)]
24. Iacono, S.T.; Jennings, A.R. Recent studies on fluorinated silica nanometer-sized particles. *Nanomaterials* **2019**, *9*, 684. [[CrossRef](#)]
25. Brassard, J.-D.; Sarkar, D.K.; Perron, J. Fluorine based superhydrophobic coatings. *Appl. Sci.* **2012**, *2*, 453–464. [[CrossRef](#)]
26. Xue, C.-H.; Zhang, Z.-D.; Zhang, J.; Jia, S.-T. Lasting and self-healing superhydrophobic surfaces by coating of polystyrene/SiO₂ nanoparticles and polydimethylsiloxane. *J. Mater. Chem A* **2014**, *2*, 15001–15007. [[CrossRef](#)]
27. Li, Z.; Cao, M.; Li, P.; Zhao, Y.; Bai, H.; Wu, Y.; Jiang, L. Surface-embedding of functional micro-/nanoparticles for achieving versatile superhydrophobic interfaces. *Matter* **2019**, *1*, 661–673. [[CrossRef](#)]
28. Si, Y.; Guo, Z.; Liu, W. A robust epoxy resins@ stearic acid-Mg(OH)₂ micronanosheet superhydrophobic omnipotent protective coating for real-life applications. *ACS Appl. Mater. Interfaces* **2016**, *8*, 16511–16520. [[CrossRef](#)]
29. Irani, F.; Jannesari, A.; Bastani, S. Effect of fluorination of multiwalled carbon nanotubes (MWCNTs) on the surface properties of fouling-release silicone/MWCNTs coatings. *Prog. Org. Coat.* **2013**, *76*, 375–383. [[CrossRef](#)]
30. Hozumi, A.; Takai, O. Preparation of ultra water-repellent films by microwave plasma-enhanced CVD. *Thin Solid Films* **1997**, *303*, 222–225. [[CrossRef](#)]
31. Sarkar, D.; Brassard, D.; El Khakani, M.; Ouellet, L. Dielectric properties of sol–gel derived high-k titanium silicate thin films. *Thin Solid Films* **2007**, *515*, 4788–4793. [[CrossRef](#)]
32. Teshima, K.; Sugimura, H.; Inoue, Y.; Takai, O. Gas barrier performance of surface-modified silica films with grafted organosilane molecules. *Langmuir* **2003**, *19*, 8331–8334. [[CrossRef](#)]
33. Zhao, Y.; Li, M.; Lu, Q.; Shi, Z. Superhydrophobic polyimide films with a hierarchical topography: Combined replica molding and layer-by-layer assembly. *Langmuir* **2008**, *24*, 12651–12657. [[CrossRef](#)] [[PubMed](#)]
34. Yu, Z.-J.; Yang, J.; Wan, F.; Ge, Q.; Yang, L.-L.; Ding, Z.-L.; Yang, D.-Q.; Sacher, E.; Isimjan, T.T. How to repel hot water from a superhydrophobic surface? *J. Mater. Chem. A* **2014**, *2*, 10639–10646. [[CrossRef](#)]



© 2020 by the authors. Licensee MDPI, Basel, Switzerland. This article is an open access article distributed under the terms and conditions of the Creative Commons Attribution (CC BY) license (<http://creativecommons.org/licenses/by/4.0/>).